

# Solutions to Buoyancy-driven Flow Problem in Square Cavity on Irregular Grids

Somchart Chantasiriwan

Faculty of Engineering, Thammasat University, Rangsit Campus, Pathum Thani 12121

## Abstract

A well-known benchmark problem modeled by the Navier-Stokes equations is the buoyancy-driven flow problem in square cavity, of which two horizontal sides are insulated and two vertical sides are kept at two different temperatures. Previously, the finite difference method has been successfully used to solve this problem. However, extension of the finite difference method to more complicated domain may be difficult. In this paper, a mesh-less method that can work on irregular grid is proposed as an alternative method for this problem. This method is used to solve the problem in the stream function-vorticity formulation. It is shown that the accuracy of the solution depends on the implementation of the vorticity boundary condition. Two schemes for discretizing the vorticity boundary condition in this formulation are proposed. The scheme that expresses boundary vorticity in terms of derivatives of stream function and velocity is shown to produce more accurate solutions than the scheme that expresses boundary vorticity in terms of derivatives of stream function.

Keywords : Navier-Stokes, natural convection, meshless, multiquadrics

## 1. Introduction

The finite difference method is an efficient method for problems having simple domain shapes. When the problem domain is irregular, however, the implementation of the finite difference method may be awkward. Although the finite element method can handle complex problem domains better, this method has its own disadvantages that include the requirements of mesh generation and the weak-form formulation of the problem. Recently, a number of alternative methods known as meshless methods have gained interest in the research community [1]. These methods do not require time-consuming mesh generation, and have been shown to be capable of solving various computational mechanics problems. Meshless methods known as point interpolation methods are analogous to the finite difference method in that they approximate a partial derivative of a function in terms of functional values at neighboring nodes. Different point interpolation methods use different functions as interpolation functions. When the interpolation function is the radial basis function known as multiquadrics, the method is known as the local

multiquadric collocation method [2]. This method has been used to solve certain linear and nonlinear problems [2–4]. The natural convection problem in a square cavity with two horizontal sides insulated and two vertical sides maintained at two different temperatures is to be referred to in this paper as the buoyancy-driven flow problem in square cavity. Although this problem is simple to describe and formulate, it does not have the analytical solution. Its simplicity makes it a popular problem for testing numerical methods. The buoyancy-driven flow problem in square cavity may be solved in one of the three well-known formulations: the primitive-variable formulation, the velocity-vorticity formulation, and the stream function-vorticity formulation. The stream function-vorticity formulation is the simplest because it contains only three dependent variables: stream function, vorticity and temperature. Since the boundary condition of the problem is usually not directly specified in terms of vorticity, this formulation must incorporate a scheme for computing boundary vorticity, which may influence the accuracy of the solution significantly. Boundary vorticity may be

expressed in terms of stream variables, vorticity or velocity components at the boundary and nearby nodes [5 – 7].

This paper is concerned with the implementation of the local multiquadric collocation method for solving the buoyancy-driven flow problem. First, details of the discretization of the governing equations and boundary conditions will be described. Then the local multiquadric collocation method for solving these equations will be presented. Two different schemes for computing boundary vorticity will be considered. The first scheme expresses boundary vorticity in terms of stream functions values, and the second scheme expresses boundary vorticity in terms of boundary velocity components and stream functions. It will be demonstrated that accurate solutions on irregular grids can be obtained by using the local multiquadric collocation method. Furthermore, it will be shown that the second scheme for computing boundary vorticity yields more accurate solutions than the first scheme.

## 2. Governing Equations and Boundary Conditions

The two-dimensional natural convection is governed by the following continuity, momentum and energy equations:

$$\frac{\partial u'}{\partial x'} + \frac{\partial v'}{\partial y'} = 0 \quad (1)$$

$$\rho \left( \frac{\partial u'}{\partial t'} + u' \frac{\partial u'}{\partial x'} + v' \frac{\partial u'}{\partial y'} \right) = -\frac{\partial p}{\partial x'} + \mu \left( \frac{\partial^2 u'}{\partial x'^2} + \frac{\partial^2 u'}{\partial y'^2} \right) \quad (2)$$

$$\rho \left( \frac{\partial v'}{\partial t'} + u' \frac{\partial v'}{\partial x'} + v' \frac{\partial v'}{\partial y'} \right) = -\frac{\partial p}{\partial y'} + \mu \left( \frac{\partial^2 v'}{\partial x'^2} + \frac{\partial^2 v'}{\partial y'^2} \right) - \rho g \quad (3)$$

$$\frac{\partial T'}{\partial t'} + u' \frac{\partial T'}{\partial x'} + v' \frac{\partial T'}{\partial y'} = \alpha \left( \frac{\partial^2 T'}{\partial x'^2} + \frac{\partial^2 T'}{\partial y'^2} \right) \quad (4)$$

where  $\rho$  is density,  $\mu$  is dynamic viscosity,  $\alpha$  is thermal diffusivity, and  $g$  is gravitational acceleration. Initially, the

fluid temperature is uniformly  $T_0$ . At time  $t' > 0$ , part of the boundary is subjected to isothermal boundary condition  $T_w$ , part of boundary is kept at the initial temperature, and the other part of the boundary is insulated.

In Boussinesq approximation,  $\rho$  is assumed to be constant in Eqs. (2) and (3) except in the source term of Eq. (3), where  $\rho$  is approximated as

$$\rho = \rho_0 - \rho\beta(T' - T_0) \quad (5)$$

and thermal expansion coefficient  $\beta$  is defined as

$$\beta = -\frac{1}{\rho} \left( \frac{\partial \rho}{\partial T} \right)_p \quad (6)$$

Insert  $\rho$  from Eq. (5) into the source term of Eq. (3), and combine the resulting equation with Eqs. (1) and (2) into two equations of stream function ( $\Psi'$ ) and vorticity ( $\omega'$ ):

$$\frac{\partial^2 \Psi'}{\partial x'^2} + \frac{\partial^2 \Psi'}{\partial y'^2} = -\omega' \quad (7)$$

$$\rho \left( \frac{\partial \omega'}{\partial t'} + \frac{\partial \Psi'}{\partial y'} \frac{\partial \omega'}{\partial x'} - \frac{\partial \Psi'}{\partial x'} \frac{\partial \omega'}{\partial y'} \right) = \mu \left( \frac{\partial^2 \omega'}{\partial x'^2} + \frac{\partial^2 \omega'}{\partial y'^2} \right) + \rho g \beta \frac{\partial (T' - T_0)}{\partial x'} \quad (8)$$

and Eq. (4) can be rewritten as

$$\frac{\partial T'}{\partial t'} + \frac{\partial \Psi'}{\partial y'} \frac{\partial T'}{\partial x'} - \frac{\partial \Psi'}{\partial x'} \frac{\partial T'}{\partial y'} = \alpha \left( \frac{\partial^2 T'}{\partial x'^2} + \frac{\partial^2 T'}{\partial y'^2} \right) \quad (9)$$

where

$$\omega' = \frac{\partial v'}{\partial x'} - \frac{\partial u'}{\partial y'} \quad (10)$$

$$u' = \frac{\partial \Psi'}{\partial y'} \quad (11)$$

$$v' = -\frac{\partial \Psi'}{\partial x'} \quad (12)$$

Assume that  $L$  is the characteristic length scale for the problem. Let's define the following dimensionless variables:  $x = x'/L$ ,  $y = y'/L$ ,  $t = \alpha t'/L^2$ ,  $u = u'L/\alpha$ ,  $v = v'L/\alpha$ ,  $T = (T' - T_0)/(T_w - T_0)$ ,  $\omega = \alpha \omega'/L^2$ , and  $\Psi = \Psi'/\alpha$ .

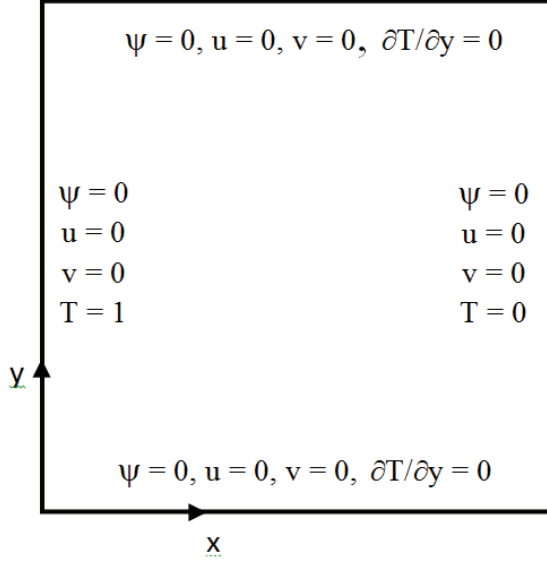


Figure 1 Boundary conditions for the buoyancy-driven flow problem in a square cavity of unit width.

Equations (7)–(9) may be written in dimensionless forms as

$$\frac{\partial^2 \Psi}{\partial x^2} + \frac{\partial^2 \Psi}{\partial y^2} = -\omega \quad (13)$$

$$\frac{\partial \omega}{\partial t} + \frac{\partial \Psi}{\partial y} \frac{\partial \omega}{\partial x} - \frac{\partial \Psi}{\partial x} \frac{\partial \omega}{\partial y} = \text{Pr} \left( \frac{\partial^2 \omega}{\partial x^2} + \frac{\partial^2 \omega}{\partial y^2} \right) + \text{Ra Pr} \frac{\partial T}{\partial x} \quad (14)$$

$$\frac{\partial T}{\partial t} + \frac{\partial \Psi}{\partial y} \frac{\partial T}{\partial x} - \frac{\partial \Psi}{\partial x} \frac{\partial T}{\partial y} = \frac{\partial^2 T}{\partial x^2} + \frac{\partial^2 T}{\partial y^2} \quad (15)$$

where Rayleigh number is  $R_a = g\beta(T_w - T_0)L^3/\nu\alpha$ , and Prandtl number is  $\text{Pr} = \nu/\alpha$ . The dimensionless problem of natural convection the square cavity of unit width is illustrated in Fig. 1. It can be seen from Fig. 1 that boundary conditions for  $T$  and  $\Psi$  are completely specified. Boundary condition for  $\omega$  is not specified, and must be determined from other variables.

### 3. Local Multiquadric Collocation Method

Let node 1 be where a partial derivative of a function  $f$  is to be discretized. Consider a group of  $n$  interpolation

nodes, which include node 1 and other  $n - 1$  nodes that may be selected by their proximity to node 1 or by another criterion. A given function value at each node may be approximated by

$$f(x_i, y_i) = \sum_{j=1}^n a_j \phi_j \quad (16)$$

where

$$\phi_{ij} = \sqrt{(x_i - x_j)^2 + (y_i - y_j)^2 + c^2} \quad (17)$$

is the radial basis function known as multiquadrics. The constant  $c$  is the shape parameter. Equation (16) is a component of the matrix equation,

$$\vec{f} = \Phi \vec{a} \quad (18)$$

which can be solved for the vector of coefficients.

$$\vec{a} = \Phi^{-1} \vec{f} \quad (19)$$

Once  $\vec{a}$  has been determined, the approximation of a partial derivative of  $f$  with respect to  $x$  or  $y$  can be expressed in terms of function values at all nodes. For example,

$$\frac{\partial \vec{f}}{\partial x} = \frac{\partial \Phi}{\partial x} \vec{a} \quad (20)$$

can be written as

$$\frac{\partial \vec{f}}{\partial x} = \left( \frac{\partial \Phi}{\partial x} \Phi^{-1} \right) \vec{f} \quad (21)$$

The first row of this matrix equation is thus the desired discretization of the partial derivative of  $f$  with respect to  $x$  at node 1. Therefore, this method can be used to express partial derivatives of  $f$  at any node  $i$  in terms of values of  $f$  at node  $i$  and  $n-1$  other nodes.

$$\left( \frac{\partial f}{\partial x} \right)_i = \sum a_{\bar{j}} f_j \quad (22)$$

$$\left( \frac{\partial f}{\partial y} \right)_i = \sum b_{\bar{j}} f_j \quad (23)$$

$$\left( \frac{\partial^2 f}{\partial x^2} \right)_i = \sum c_{\bar{j}} f_j \quad (24)$$

$$\left( \frac{\partial^2 f}{\partial y^2} \right)_i = \sum d_{\bar{j}} f_j \quad (25)$$

Right hand sides of Eqs. (22) – (25) are summations over all nodes  $j$  in the domain. It should be noted that, in each of Eqs. (22) – (25), most of coefficients are zero except for the  $n$  coefficients at corresponding  $n$  selected nodes.

Discretization of Eqs. (12) – (14) at an interior node  $i$  using the local multiquadric collocation method and the implicit time-stepping scheme results in the following nonlinear algebraic equations:

$$\sum c_{\bar{j}} \psi_j^{(m)} + \sum d_j \psi_j^{(m)} = -\omega_i^{(m)} \quad (26)$$

$$\begin{aligned} & \left( \frac{\omega_i^{(m)} - \omega_i^{(m-1)}}{\Delta t} \right) + \left( \sum b_j \psi_j^{(m)} \right) \left( \sum a_j \omega_j^{(m)} \right) \\ & - \left( \sum a_{\bar{j}} \psi_j^{(m)} \right) \left( \sum b_j \omega_j^{(m)} \right) \\ = & \text{Pr} \left( \sum c_{ij} \omega_j^{(m)} + \sum d_{ij} \omega_j^{(m)} \right) + \text{Ra Pr} \sum a_{ij} T_j^{(m)} \quad (27) \end{aligned}$$

$$\begin{aligned} & \left( \frac{T_i^{(m)} - T_i^{(m-1)}}{\Delta t} \right) + \left( \sum b_j \psi_j^{(m)} \right) \left( \sum a_j T_j^{(m)} \right) \\ & - \left( \sum a_{\bar{j}} \psi_j^{(m)} \right) \left( \sum b_j T_j^{(m)} \right) \\ = & \sum c_{\bar{j}} T_j^{(m)} + \sum d_j T_j^{(m)} \quad (28) \end{aligned}$$

where superscript  $m$  denotes value at time  $m\Delta t$ . In addition to Eqs. (26) – (28), discretized boundary conditions for  $\psi$ ,  $T$ , and  $\omega$  are needed. According to Fig. 1,

$$\psi_i^{(m)} = 0 \quad (29)$$

for any boundary node  $i$ ,

$$T_i^{(m)} = 1 \quad (30a)$$

for boundary node  $i$  on the left wall,

$$T_i^{(m)} = 0 \quad (30b)$$

for boundary node  $i$  on the right wall

$$T_i^{(m)} = - \frac{\sum_{j \neq i} b_{\bar{j}} T_j^{(m)}}{b_i} \quad (30c)$$

for boundary node  $i$  on the horizontal walls.

For the purpose of computing vorticity at boundary node  $i$ ,  $n - 1$  interior nodes that are nearest to node  $i$  are selected as shown in Fig. 2. Two schemes for determining the vorticity boundary condition are considered here. The

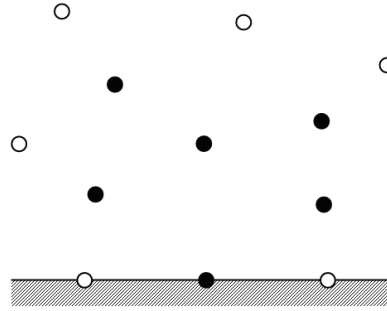


Figure 2 Six nodes (designated by solid circles) used for discretization of the vorticity boundary condition.

first scheme uses the relation between  $\omega$  and  $\psi$  from Eq. (13), which results in

$$\omega_i^{(m)} = - \sum c_{\bar{j}} \psi_j^{(m)} \quad (31a)$$

on the vertical walls,

$$\omega_i^{(m)} = - \sum d_{\bar{j}} \psi_j^{(m)} \quad (31b)$$

on the horizontal walls. The second scheme uses the relation between  $\omega$  and velocity components from Eq. (10), which results in

$$\omega_i^{(m)} = \sum a_{\bar{j}} v_j^{(m)} \quad (32a)$$

on the vertical walls,

$$\omega_i^{(m)} = - \sum b_{\bar{j}} u_j^{(m)} \quad (32b)$$

on the horizontal walls because boundary velocity is zero. Velocity components at interior node  $j$  in Eq. (32) are computed from Eqs. (11) and (12).

$$u_j^{(m)} = \sum b_{\bar{k}} \psi_k^{(m)} \quad (33)$$

$$v_j^{(m)} = - \sum a_{\bar{k}} \psi_k^{(m)} \quad (34)$$

The system of equations formed by Eqs. (26) – (30) and either Eq. (31) or Eqs. (32) – (34) must be solved by iteration. The iteration process starts with  $\psi_i^{(0)} = T_i^{(0)} = \omega_i^{(0)} = 0$  at interior nodes. The successive overrelaxation method (SOR) is then used to find  $\psi_i^{(l)}$ ,  $T_i^{(l)}$ ,  $\omega_i^{(l)}$ . The iteration process is continued until convergence when the solution reaches the steady state.

#### 4. Benchmark Solutions

Since exact solutions of the buoyancy-driven flow problem in square cavity are not available, numerical solutions by the multiquadric collocation method must be compared with the benchmark solutions. Erturk and Gokcol [8] solved to the lid-driven flow problem by the finite difference method. They obtained highly accurate solutions by using the vorticity boundary condition suggested by Stortkuhl et al. [6]. Their Fortran codes are available at the website <http://www.cavityflow.com>. These codes were modified by the author of this paper to solve the buoyancy-driven flow problem in square cavity. Results on  $161 \times 161$  grid obtained for velocity components ( $u$  and  $v$ ) and heat flux ( $q = \partial T / \partial x$ ) at selected points are considered to be benchmark solutions. Figure 3 shows these results for  $Pr = 0.7$  and  $Ra = 1000, 10000, \text{ and } 100000$ .

#### 5. Results and Discussion

As mentioned earlier, one advantage of the local multiquadric collocation method and most other meshless methods is the freedom to place nodes randomly in the domain. A random node arrangement is created by positioning each interior node  $i$  at  $(x_i, y_i) = (x_{0i} + 0.3r_1\Delta, y_{0i} + 0.3r_2\Delta)$ , where  $(x_{0i}, y_{0i})$  is the position of node  $i$  in the uniform arrangement in the square grid having  $\Delta$  as the grid spacing, and  $r_1$  and  $r_2$  are random numbers between  $-0.5$  and  $0.5$ . Note that  $\Delta = 1/(\sqrt{N} - 1)$ , where  $N$  is the total number of nodes. The number of nodes ( $n$ ) used for collocation is 6.

It is found that solutions to the buoyancy-driven flow problem by the local multiquadric collocation method on irregular grids are satisfactorily accurate because these solutions produce similar distributions of  $u, v,$  and  $q$  to the distributions shown in Fig. 3. For the purpose of assessing the degree of accuracy, it is useful to define error as the absolute value of the difference between the solution by the local multiquadric collocation method ( $f$ ) and the benchmark solution ( $f_c$ ) divided by  $f_c$ :

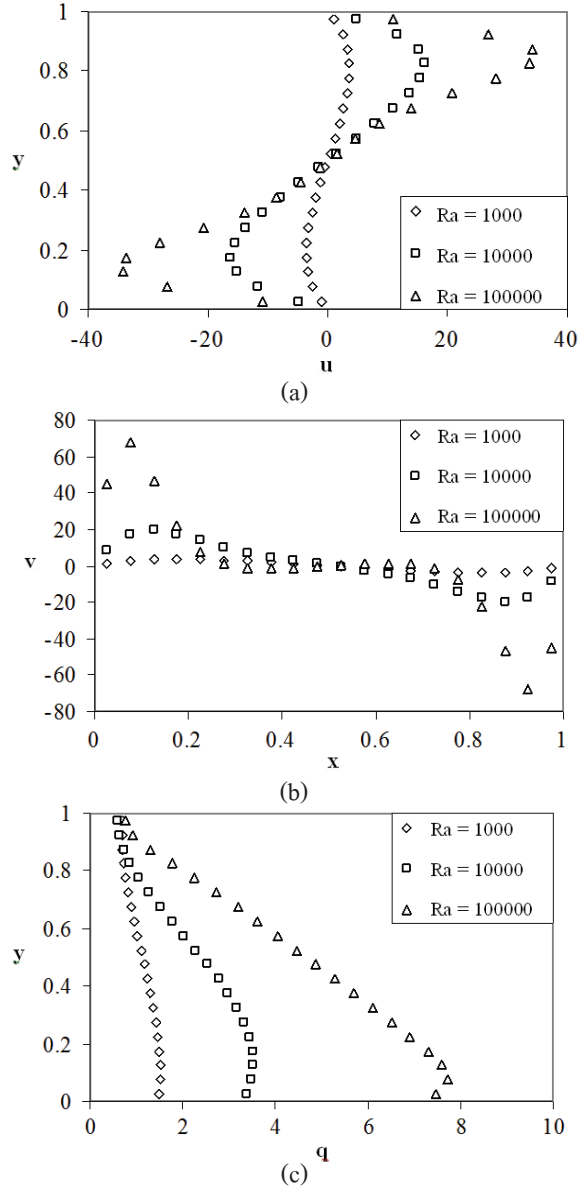


Figure 3 Distributions of (a) the horizontal velocity component along the vertical line passing the center of the square cavity; (b) the vertical velocity component along the horizontal line passing the center of the square cavity; and (c) the heat flux along the left wall of the square cavity for  $Ra = 1000, 10000, \text{ and } 100000$  from the benchmark solutions.

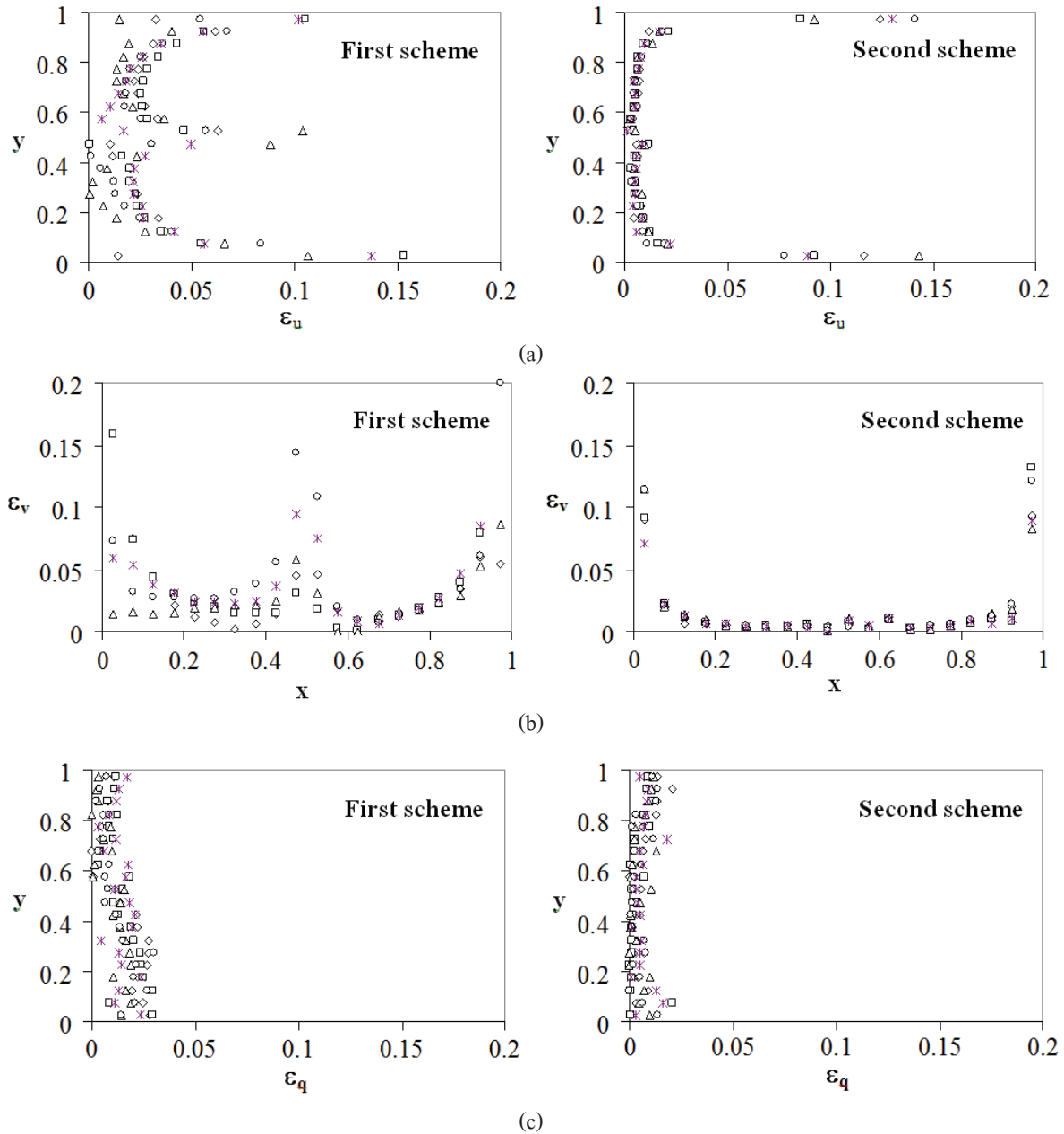


Figure 4 Comparison between errors in (a) the horizontal velocity component; (b) the vertical velocity component; and (c) the heat flux of solutions by the local multiquadric collocation method for  $Pr = 0.7$  and  $Ra = 1000$  that use the first scheme and the second scheme of discretizing the vorticity boundary condition.

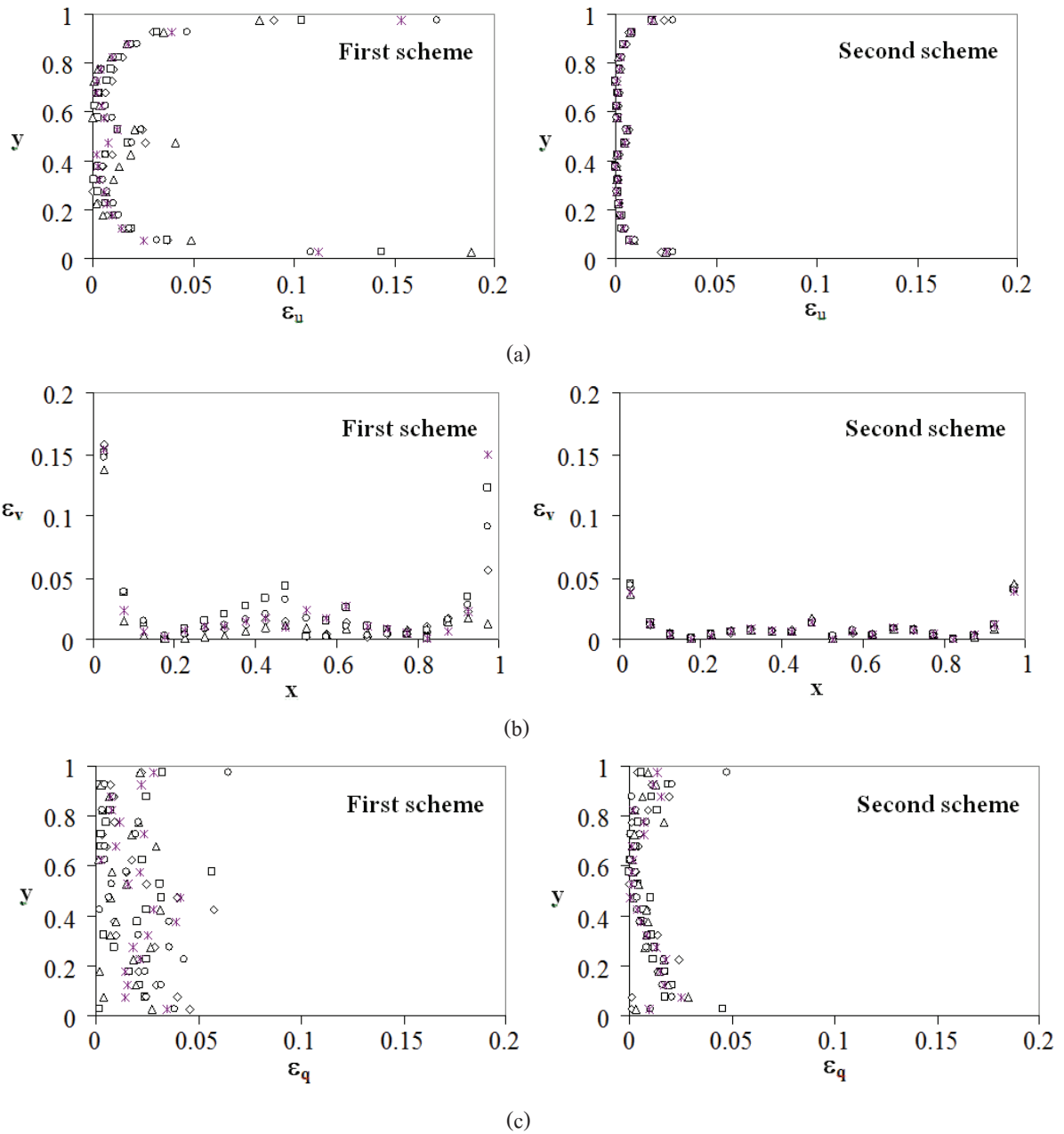


Figure 5 Comparison between errors in (a) the horizontal velocity component; (b) the vertical velocity component; and (c) the heat flux of solutions by the local multiquadric collocation method for  $Pr = 0.7$  and  $Ra = 10000$  that use the first scheme and the second scheme of discretizing the vorticity boundary condition.

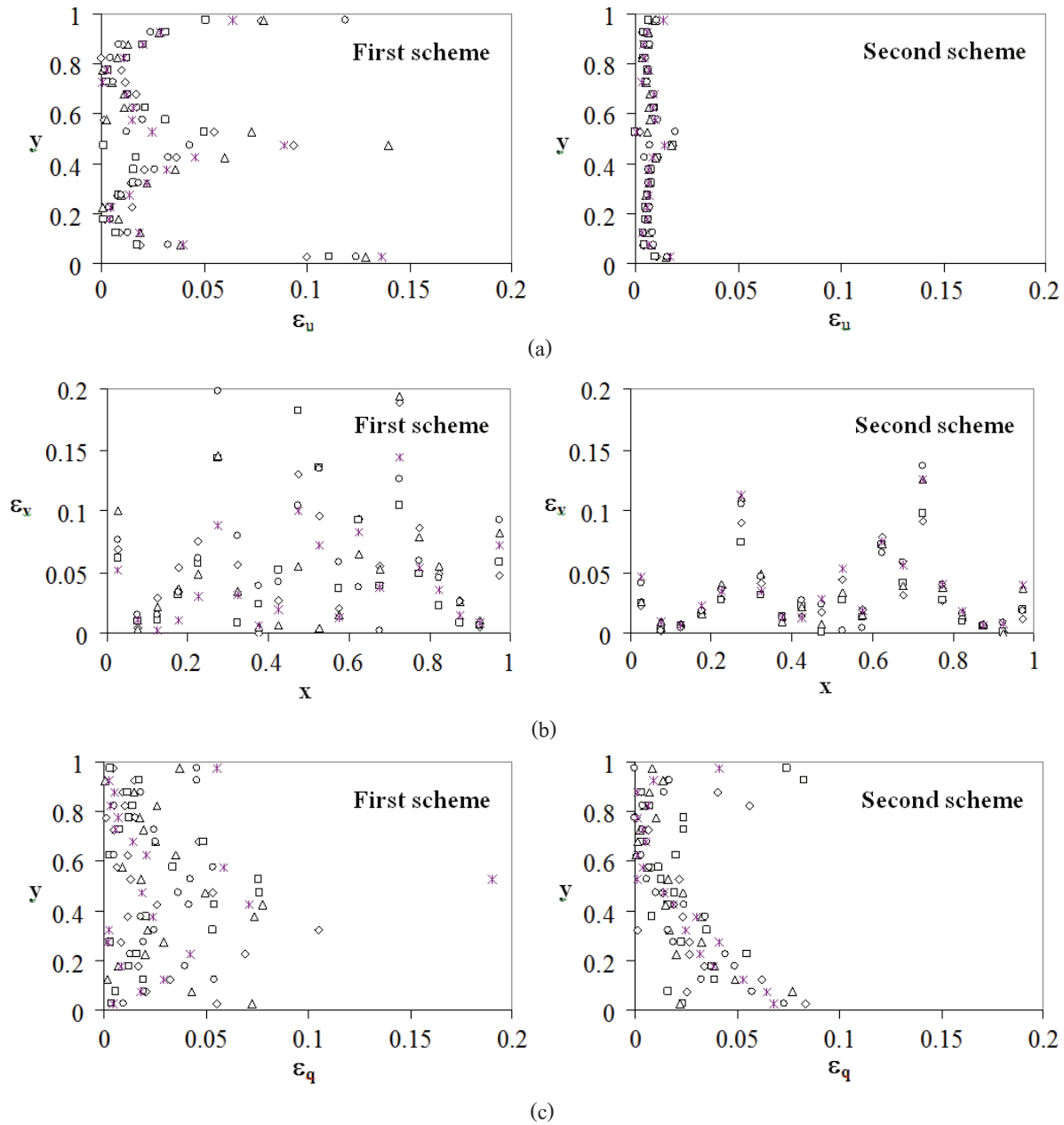


Figure 6 Comparison between errors in (a) the horizontal velocity component; (b) the vertical velocity component; and (c) the heat flux of solutions by the local multiquadric collocation method for  $Pr = 0.7$  and  $Ra = 100000$  that use the first scheme and the second scheme of discretizing the vorticity boundary condition.

$$\varepsilon_r = \left| \frac{f - f_e}{f_e} \right| \quad (35)$$

where  $f$  represents  $u$ ,  $v$ , or  $q$ . Errors of solutions by the local multiquadric collocation method are computed for  $Pr = 0.7$  and  $Ra = 1000, 10000, \text{ and } 100000$  on five random node arrangements. Solutions are produced in two sets, which use two schemes for determining the vorticity boundary condition. The first scheme uses Eq. (31), whereas the second scheme uses Eqs. (32) – (34).

Figures 4 – 6 show distributions of  $\varepsilon_u$ ,  $\varepsilon_v$ , and  $\varepsilon_q$  for  $Ra = 1000, 10000, \text{ and } 100000$ , respectively. In each figure, different symbol represents different random node arrangement. The number of nodes used to obtain results in Fig. 4 is 1681. Since higher  $Ra$  requires more nodes to obtain solutions of comparable accuracy, the numbers of nodes used to obtain results in Fig. 5 and 6 are 3721 and 6561, respectively. It can be seen that all five random node arrangements yield satisfactorily accurate solutions when either the first or the second scheme for determining the vorticity boundary condition is used. Comparisons of both schemes reveal that the second scheme produces more accurate solutions than the first scheme. It should be noted that solutions are less accurate near the sides of the cavity and near the center of the cavity.

Previous works [2, 4] indicate that the accuracy of the local multiquadric collocation method in solving certain linear problems is relatively insensitive to the shape parameter  $c$  in Eq. (17), but can be improved by decreasing  $\Delta$  or increasing  $n$ . It is found that the accuracy of the local multiquadric collocation method in solving the buoyancy-driven flow problem can be increased by decreasing  $\Delta$ . Although increasing  $n$  may result in more accurate solutions for linear problems, it may not result in more accurate solutions for nonlinear problems because converged solutions may not be found. It is therefore suggested that, as far as nonlinear problems are concerned,  $n$  should be kept at 6 so that the iteration process leads to convergence. If more

accurate solutions are desired, smaller  $\Delta$  should be used.

## 6. Conclusions

The buoyancy-driven flow problem in square cavity, of which two horizontal sides are insulated and two vertical sides are kept at two different temperatures, is solved by a meshless method known as the local multiquadric collocation method. Two schemes for discretizing the vorticity boundary condition are considered. The first scheme expresses boundary vorticity in terms of derivatives of stream function, whereas the second one expresses boundary vorticity in terms of derivatives of stream function and velocity. Solutions by the local multiquadric collocation method on irregular grids are compared with the benchmark solutions for  $Pr = 0.7$  and  $Ra = 1000, 10000, \text{ and } 10000$ . It is found that both schemes can yield accurate solutions, and that errors of solutions in the second scheme are less than those in the first scheme.

## 7. References

- [1] Liu GR. Mesh Free Methods: Moving Beyond the Finite Element Method. CRC Press: Boca Raton; 2003.
- [2] Chantasiriwan S. Investigation of the use of radial basis functions in local collocation method for solving diffusion problems. *International Communications in Heat and Mass Transfer*. 2004; 31(8): 1095-1104.
- [3] Chantasiriwan S. Solutions to harmonic and biharmonic problems with discontinuous boundary conditions by collocation methods using multiquadrics as basis functions. *International Communications in Heat and Mass Transfer*. 2007; 34(3): 313-320.
- [4] Lee CK, Liu X, Fan, SC. Local multiquadric approximation for solving boundary value problems. *Computational Mechanics*. 2003; 30(5-6): 396-409.
- [5] Gupta MM. High accuracy solutions of incompressible Navier-Stokes equations. *Journal of Computational Physics*. 1991; 93(2): 343-359.
- [6] Stoerkuhl T, Zenger C, Zimmer S. An asymptotic

- solution for the singularity at the angular point of the lid driven cavity. *International Journal of Numerical Methods for Heat & Fluid Flow*. 1994: 4(1), 47-59.
- [7] Weinan E, and Liu J-G. Vorticity boundary condition and related issues for finite difference schemes. *Journal of Computational Physics*. 1996: 124(2), 368-382.
- [8] Erturk E, Gokcol C. Fourth order compact formulation of Navier-Stokes equations and driven cavity flow at high Reynolds numbers. *International Journal for Numerical Methods in Fluids*. 2006: 50(6), 421-436.